Acta Crystallographica Section A
Foundations of Crystallography
ISSN 0108-7673

Received 6 October 2008
Accepted 9 December 2008

A general approach for determining the diffraction contrast factor of straight-line dislocations

Jorge Martinez-Garcia,[a,b]* Matteo Leoni[b] and Paolo Scardi[b]

[a]École Polytechnique Fédérale de Lausanne (EPFL), Laboratoire de Cristallographie, BSP, CH-1015 Lausanne, Switzerland, and [b]Department of Materials Engineering and Industrial Technologies, University of Trento, via Mesiano 77, Trento 38100, Italy. Correspondence e-mail: jorge.martinezgarcia@epfl.ch

Dislocations alter perfect crystalline order and produce anisotropic broadening of the X-ray diffraction profiles, which is described by the dislocation contrast factor. Owing to the lack of suitable mathematical tools to deal with dislocations in crystals of any symmetry, contrast factors are so far only known for a few slip systems in high-symmetry phases and little detail is given in the literature on the calculation procedure. In the present paper a general approach is presented for the calculation of contrast factors for any dislocation configuration and any lattice symmetry. The new procedure is illustrated with practical examples of hexagonal metals and some low-symmetry mineral phases.

1. Introduction

The interest in dislocation effects on diffraction-line broadening dates back to the pioneering work of Wilson, whose theoretical investigations started even before there was direct evidence of the existence of dislocations (Wilson, 1949, 1950). From then on, the local atomic displacement produced by the dislocation strain field was recognized as one of the main sources of 'strain broadening' of the line profiles.

The possibility of modeling dislocation effects and in particular of separating their contribution from that of the crystalline domain size was well established in the 1950s (Williamson & Hall, 1953). However, Krivoglaz first realized the importance of the distribution of dislocations in the early 1960s (Krivoglaz & Ryaboshapka, 1963): dislocation effects cannot be described by considering the effect of the closest dislocations only (Wilson, 1949, 1950), but proper account is required for the displacement due to – virtually – all dislocations in the crystal, including their arrangement, interaction and orientation (Krivoglaz & Ryaboshapka, 1963; Krivoglaz *et al.*, 1983).

Further developments were proposed by Wilkens in the late 1960s (Wilkens, 1970*a*,*b*), leading to the Krivoglaz–Wilkens (KW) theory which is nowadays considered the standard for studying dislocation effects in diffraction-line profile analysis (LPA) [see *e.g.* Mittemeijer & Scardi (2004) and references therein]. According to the KW theory, the Fourier transform of a peak profile depends on the Burgers vector $\mathbf{b}_{\rm v}$ of a given $\langle UVW\rangle\{HKL\}$ slip system, on the dislocation density ρ, on the arrangement parameter $R_{\rm e}$ (effective outer cut-off radius), and on the so-called contrast (or orientation) factor C_{hkl} (Wilkens, 1970*a*,*b*). The latter is the main parameter describing the effect of the dislocation strain field projected along the diffraction scattering direction (Armstrong *et al.*, 2006), *i.e.*, the way dislocations are 'seen' through diffraction.

Any practical application of the KW theory requires contrast-factor calculations for the specific slip system and elastic medium, a rather complex numerical procedure if elastic anisotropy is considered. Contrast-factor calculation was pioneered by Krivoglaz and Ryaboshapka, who discussed the elastically isotropic case (Krivoglaz & Ryaboshapka, 1963) [mistakes in the original 1963 paper were corrected in Krivoglaz *et al.* (1983)]. The importance of considering elastic anisotropy was recognized by Ryaboshapka (1965), but a comprehensive compilation of contrast factors appeared only in 1987, for the specific case of copper (Wilkens, 1987).

The first procedure for contrast-factor calculation in highly symmetric lattices was proposed at the end of the 1980s by Klimanek and Kužel (KK) (Klimanek & Kužel, 1988; Kužel & Klimanek, 1988), and can be considered as the only relevant theoretical contribution in this field until the end of the 20th century. In the following years, several collections of contrast factors obtained by the KK procedure were proposed (Ungár *et al.*, 1999; Dragomir & Ungár, 2002*a*,*b*; Borbély *et al.*, 2003), but in most cases little detail of the calculation procedure was given. More recently, Armstrong & Lynch (2004) made an effort to clarify the calculation methodology, illustrating the KK procedure step-by-step for some examples of face-centered and body-centered cubic materials. Differences among results in the various papers can be attributed to errors [some of which are discussed in Martinez-Garcia (2008)] and different numerical approximations.

The present paper can be considered as a generalization of previous work (Krivoglaz & Ryaboshapka, 1963; Krivoglaz *et al.*, 1983; Wilkens, 1970*a*,*b*, 1987; Klimanek & Kužel, 1988; Kužel & Klimanek, 1988; Armstrong & Lynch, 2004) for calculating contrast factors for any slip system and crystallographic symmetry in elastically anisotropic crystals and polycrystals. The proposed procedure is here illustrated by applications to some hexagonal metals and to low-symmetry mineral phases. It can be included in state-of-the-art LPA methods and used to extract dislocation parameters from broadened X-ray diffraction profiles.

2. Mathematical background

2.1. General coordinate systems and their relationships

Three reference systems, shown in Fig. 1 and described in the following, are conveniently introduced for contrast-factor calculations, namely the dislocation slip system $S\{\mathbf{e}_k;\, k = 1, 2, 3\}$, the crystal lattice $C\{\mathbf{a}, \mathbf{b}, \mathbf{c}\}$ and an orthonormal frame $O\{\mathbf{i}, \mathbf{j}, \mathbf{k}\}$.

Dislocation strain field calculations are done in S, suitably writing the $\{\mathbf{e}_k;\, k = 1, 2, 3\}$ basis in terms of the unit-cell parameters $\{a, b, c, \alpha, \beta, \gamma\}$. The common orthonormal frame O is employed, written in terms of $\mathbf{a}, \mathbf{b}, \mathbf{c}$ as $\mathbf{i} = \mathbf{a}/a$, $\mathbf{j} = \mathbf{k} \times \mathbf{i}$ and $\mathbf{k} = \mathbf{c}^*/c^*$ ($*$ denotes reciprocal-lattice quantities), or equivalently as

$$\begin{bmatrix} \mathbf{i} \\ \mathbf{j} \\ \mathbf{k} \end{bmatrix} = M \begin{bmatrix} \mathbf{a} \\ \mathbf{b} \\ \mathbf{c} \end{bmatrix}, \tag{1}$$

where the matrix

$$M = \begin{bmatrix} 1/a & 0 & 0 \\ -\cos(\gamma)/[a\sin(\gamma)] & 1/[b\sin(\gamma)] & 0 \\ a^*\cos(\beta^*) & b^*\cos(\alpha^*) & c^* \end{bmatrix}$$

obeys the relation $G_{\rm m} = M^{-1}(M^{-1})^T = M^{-1}(M^T)^{-1}$, $G_{\rm m}$ being the metric tensor of the crystal lattice,

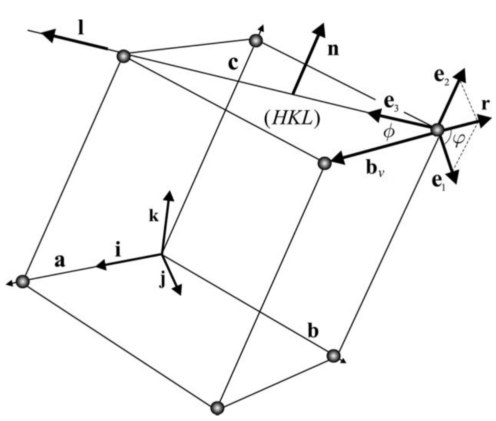

Figure 1
Unit cell of a general crystal with a straight dislocation ($\mathbf{b}_{\rm v}, \mathbf{l}$), identified in both the crystallographic C and orthogonal O frames ($\{\mathbf{a}, \mathbf{b}, \mathbf{c}\}$ and $\{\mathbf{i}, \mathbf{j}, \mathbf{k}\}$, respectively). The dislocation line vector $\mathbf{l}$ lies on its slip plane (HKL) and the reciprocal vector $\mathbf{n} = H\mathbf{a}^* + K\mathbf{b}^* + L\mathbf{c}^*$ is normal to (HKL). The S reference is chosen in such a way that $\mathbf{e}_2 = \mathbf{n}/n$, $\mathbf{e}_3 = \mathbf{l}$ and $\mathbf{e}_1 = \mathbf{e}_2 \times \mathbf{e}_3$. The vector $\mathbf{l}$ is obtained by rotating the Burgers vector $\mathbf{b}_{\rm v}$ clockwise by an angle ϕ (dislocation character) around $\mathbf{e}_2$. φ denotes the polar angle of the vector $\mathbf{r}$ on the $\{\mathbf{e}_1, \mathbf{e}_2\}$ plane.

$$G_{\rm m} = \begin{bmatrix} a^2 & ab\cos(\gamma) & ac\cos(\beta) \\ ab\cos(\gamma) & b^2 & bc\cos(\alpha) \\ ac\cos(\beta) & bc\cos(\alpha) & c^2 \end{bmatrix}.$$

Let $\{\xi_i^k;\ (i,k) = 1, 2, 3\}$ be the coordinates of the unit vectors $\{\mathbf{e}_k;\ k = 1, 2, 3\}$ on $\{\mathbf{i}, \mathbf{j}, \mathbf{k}\}$. Following these conventions, slip unit vectors can be written as

$$\begin{bmatrix} \mathbf{e}_1 \\ \mathbf{e}_2 \\ \mathbf{e}_3 \end{bmatrix} = P \begin{bmatrix} \mathbf{i} \\ \mathbf{j} \\ \mathbf{k} \end{bmatrix}, \qquad P = \begin{bmatrix} \xi_1^1 & \xi_2^1 & \xi_3^1 \\ \xi_1^2 & \xi_2^2 & \xi_3^2 \\ \xi_1^3 & \xi_2^3 & \xi_3^3 \end{bmatrix}. \tag{2}$$

According to the above equation, the problem consists of finding the matrix P which transforms the basis $\{\mathbf{i}, \mathbf{j}, \mathbf{k}\}$ into $\{\mathbf{e}_1, \mathbf{e}_2, \mathbf{e}_3\}$. By knowing the dislocation slip system $(\langle UVW \rangle\{HKL\})$ and character (ϕ), the coefficients ξ_i^k of the matrix P can be determined as follows.

(*a*) The vector $\mathbf{n} = H\mathbf{a}^* + K\mathbf{b}^* + L\mathbf{c}^*$, with coordinates $[H, K, L]$ in the reciprocal basis $[\mathbf{a}^*, \mathbf{b}^*, \mathbf{c}^*]^T$, is perpendicular to the slip plane with Miller indices (HKL) (Fig. 1). The coordinates $\{\xi_j^2;\ j = 1, 2, 3\}$ of $\mathbf{e}_2$ on $\{\mathbf{i}, \mathbf{j}, \mathbf{k}\}$ can thus be determined as

$$\begin{bmatrix} \xi_1^2 \\ \xi_2^2 \\ \xi_3^2 \end{bmatrix} = \frac{1}{|\mathbf{n}|} M \begin{bmatrix} H \\ K \\ L \end{bmatrix}, \qquad |\mathbf{n}| = \left(\mathbf{n} \cdot G_{\rm m}^* \cdot \mathbf{n}^T\right)^{1/2}, \tag{3}$$

where $G_{\rm m}^* = G_{\rm m}^{-1}$ is the metric tensor of the reciprocal lattice.

(*b*) The evaluation of the coordinates $\{\xi_j^3;\ j = 1, 2, 3\}$ of $\mathbf{e}_3$ in $\{\mathbf{i}, \mathbf{j}, \mathbf{k}\}$ requires a previous reconstruction of the line direction from the slip-system data. The normalized coordinates of the Burgers vector in the orthogonal basis $\{\xi_1^b, \xi_2^b, \xi_3^b\}$ are obtained as

$$\begin{bmatrix} \xi_1^b \\ \xi_2^b \\ \xi_3^b \end{bmatrix} = \frac{1}{|\mathbf{b}_{\rm v}|} \left(M^T\right)^{-1} \begin{bmatrix} U \\ V \\ W \end{bmatrix}, \qquad |\mathbf{b}_{\rm v}| = \left(\mathbf{b}_{\rm v} \cdot G \cdot \mathbf{b}_{\rm v}^T\right)^{1/2}. \tag{4}$$

The coordinates $\{\xi_j^3;\ j = 1, 2, 3\}$ of $\mathbf{e}_3$ in O are in turn obtained after rotation of $\{\xi_1^b, \xi_2^b, \xi_3^b\}$ by an angle ϕ using the rotation matrix $R(\phi, \mathbf{e}_2)$ (Fig. 1) (Giacovazzo *et al.*, 1992),

$$\begin{bmatrix} \xi_1^3 \\ \xi_2^3 \\ \xi_3^3 \end{bmatrix} = R(\phi, \mathbf{e}_2) \begin{bmatrix} \xi_1^b \\ \xi_2^b \\ \xi_3^b \end{bmatrix}, \tag{5}$$

where

$$R(\phi, \mathbf{e}_2) = \begin{bmatrix} 2(\xi_1^2)^2\sin^2(\phi/2) + \cos(\phi) & 2\xi_1^2\xi_2^2\sin^2(\phi/2) + \xi_3^2\sin(\phi) & 2\xi_1^2\xi_3^2\sin^2(\phi/2) - \xi_2^2\sin(\phi) \\ 2\xi_1^2\xi_2^2\sin^2(\phi/2) - \xi_3^2\sin(\phi) & 2(\xi_2^2)^2\sin^2(\phi/2) + \cos(\phi) & 2\xi_2^2\xi_3^2\sin^2(\phi/2) + \xi_1^2\sin(\phi) \\ 2\xi_1^2\xi_3^2\sin^2(\phi/2) + \xi_2^2\sin(\phi) & 2\xi_2^2\xi_3^2\sin^2(\phi/2) - \xi_1^2\sin(\phi) & 2(\xi_3^2)^2\sin^2(\phi/2) + \cos(\phi) \end{bmatrix}. \tag{6}$$

(*c*) The remaining components of $\mathbf{e}_1$ on $\{\mathbf{i}, \mathbf{j}, \mathbf{k}\}$, $\{\xi_j^1; j = 1, 2, 3\}$ are obtained as the cross product of the two vectors already calculated,

$$\begin{bmatrix} \xi_1^1 \\ \xi_2^1 \\ \xi_3^1 \end{bmatrix} = \begin{vmatrix} \mathbf{i} & \mathbf{j} & \mathbf{k} \\ \xi_1^2 & \xi_2^2 & \xi_3^2 \\ \xi_1^3 & \xi_2^3 & \xi_3^3 \end{vmatrix} = \mathbf{e}_2 \times \mathbf{e}_3. \tag{7}$$

(*d*) Finally, the representation of the unit vectors $\{\mathbf{e}_i;\ i = 1, 2, 3\}$ in the *C* reference frame can be obtained as

$$\begin{bmatrix} \mathbf{e}_1 \\ \mathbf{e}_2 \\ \mathbf{e}_3 \end{bmatrix} = PM \begin{bmatrix} \mathbf{a} \\ \mathbf{b} \\ \mathbf{c} \end{bmatrix}. \tag{8}$$

This approach allows a straightforward identification of the dislocation reference frame *S* in crystals of any symmetry, through the sole use of the G_m, M and $R(\phi, \mathbf{e}_2)$ matrices carrying the metric information. This is a substantial generalization of the work of Klimanek & Kužel (1988), Kužel & Klimanek (1988) and Armstrong & Lynch (2004), leading to a simpler procedure for contrast-factor calculation.

2.2. Contrast factor for a given slip system

According to Klimanek & Kužel (1988) and Kužel & Klimanek (1988), the contrast factor can be conveniently written as the product of two 4-rank tensors, namely the geometrical G_{ijmn} and elastic E_{ijmn} components,

$$C_{hkl} = \sum_{i,m}^{3} \sum_{j,n}^{2} G_{ijmn} E_{ijmn}. \tag{9}$$

Even if equation (9) is general in character, its application has so far been limited to cubic and hexagonal crystals, due to a lack of mathematical tools for dealing with dislocations in anisotropic crystals of any symmetry. The use of equation (9) is here extended, providing general expressions for the tensors G_{ijmn} and E_{ijmn} as a function of the unit-cell parameters and elastic properties of crystals.

2.2.1. Determining G_{ijmn}. The G_{ijmn} tensor is obtained from the direction cosines, $\tau_i = (\mathbf{d}^*/d^*) \cdot \mathbf{e}_i$, of the angles between the diffraction vector and the axes of the *S* system:

$$G_{ijmn} = \tau_i \tau_j \tau_m \tau_n, \quad (i, m) = 1, 2, 3, \quad (j, n) = 1, 2. \tag{10}$$

By using the formalism introduced in the previous section, direction cosines are written as

$$\begin{aligned} \tau_2 &= \frac{[h,k,l] \cdot G_\mathrm{m}^* \cdot [H,K,L]^T}{([H,K,L] \cdot G_\mathrm{m}^* \cdot [H,K,L]^T)^{1/2} ([h,k,l] \cdot G_\mathrm{m}^* \cdot [h,k,l]^T)^{1/2}} \\ \tau_3 &= \frac{[h,k,l] \cdot M^T \cdot R(\phi, \mathbf{e}_2) \cdot [M^T]^{-1} \cdot [U,V,W]^T}{([U,V,W] \cdot G_\mathrm{m} \cdot [U,V,W]^T)^{1/2} ([h,k,l] \cdot G_\mathrm{m}^* \cdot [h,k,l]^T)^{1/2}} \\ \tau_1 &= (1 - \tau_2^2 - \tau_3^2)^{1/2}, \end{aligned} \tag{11}$$

hkl being general Miller indices.

In order to evaluate the τ_i, we thus need to know the slip plane (*HKL*), the Burgers vector [*UVW*], the dislocation character ϕ and the matrices G_m, M and $R(\phi, \mathbf{e}_2)$ carrying information on the crystal's metric.

2.2.2. Determining E_{ijmn}. The components of the elastic part of the dislocation contrast factor, E_{ijmn}, are defined by the integral

$$E_{ijmn} = (1/\pi) \int_0^{2\pi} \beta_{ij}(\varphi) \beta_{mn}(\varphi)\, \mathrm{d}\varphi, \tag{12}$$

where the quantities β_{ij} are proportional to the partial derivatives $\partial u_i / \partial x_j$ of the displacement field of the dislocation (Klimanek & Kužel, 1988) and φ is the polar angle (Fig. 1). In determining E_{ijmn} from equation (12), it is necessary first to evaluate the displacement field $\mathbf{u}$ of an isolated dislocation in an elastically anisotropic medium. Several routes for obtaining the solutions for $\mathbf{u}$ have been proposed (Lekhnitskii, 1963; Ting, 1996). However, as was demonstrated recently (Martinez-Garcia *et al.*, 2007, 2008), the Stroh formalism (Stroh, 1958, 1962; Ting, 1996) is more convenient in finding expressions for E_{ijmn}, as it provides the solution for $\mathbf{u}$ in terms of the eigenvalues p_α and the eigenvectors $(\mathbf{A}_\alpha, \mathbf{L}_\alpha)$ of a linear eigenvalue problem in the elastic constant representation. The alternative approach proposed by Lekhnitskii (1963) and Teodosiou (1982), employed previously in contrast-factor calculations, leads to complex and large-sized solutions even in the simplest cases.

In this section the Stroh formalism is used to obtain a general expression for E_{ijmn} as function of the eigensolutions of the Stroh eigenvalue problem. Although complex, p_α and $(\mathbf{A}_\alpha, \mathbf{L}_\alpha)$ can be considered as fundamental materials' constants depending on the elastic stiffness and the orientation of the dislocation line represented in the crystal reference frame *C*.

Let us write the *m*th component of the displacement field as a function of the coordinates x_1 and x_2 on the $\{\mathbf{e}_1, \mathbf{e}_2\}$ plane (Fig. 1) as

$$u_m(x_1, x_2) = (b_\mathrm{v}/2\pi) \mathrm{Im}\left[\sum_{\alpha=1}^{3} A_{m\alpha} D_\alpha \ln(x_1 + p_\alpha x_2)\right], \tag{13}$$

where

$$D_\alpha = -\frac{(\mathbf{L}_\alpha \cdot \mathbf{b}_\mathrm{v})}{b_\mathrm{v}(\mathbf{A}_\alpha \cdot \mathbf{L}_\alpha)},$$

Im[ ] denotes the imaginary part operator and $b_\mathrm{v} = |\mathbf{b}_\mathrm{v}|$ is the Burgers vector modulus.

According to equation (12), to determine E_{ijmn} the $\beta_{mn}(x_1, x_2)$ functions related to the gradient of displacement need to be calculated:

$$\beta_{mn}(x_1, x_2) = \frac{2\pi r}{b_\mathrm{v}} \frac{\partial u_m(x_1, x_2)}{\partial x_n}, \quad r = (x_1^2 + x_2^2)^{1/2}. \tag{14}$$

Provided that the logarithm is a smooth function far from the dislocation core, substitution of equation (13) into equation (14) yields

$$\beta_{mn}(x_1, x_2) = r\ \mathrm{Im}\left[\sum_{\alpha=1}^{3} A_{m\alpha} D_\alpha \frac{\partial}{\partial x_n} \ln(x_1 + p_\alpha x_2)\right]. \tag{15}$$

Performing the differentiation in equation (15) and with a subsequent transformation to polar coordinates $\{x_1 = r\cos(\varphi), x_2 = r\sin(\varphi)\}$, we find that

$$\beta_{mn}(\varphi) = \mathrm{Im}\left[\sum_{\alpha=1}^{3} \frac{A_{m\alpha} D_\alpha p_\alpha^{(n-1)}}{\cos(\varphi) + p_\alpha \sin(\varphi)}\right]. \tag{16}$$

By inserting equation (16) into equation (12), the following expression for E_{ijmn} is obtained:

$$E_{ijmn} = \sum_{\alpha,\alpha'=1}^{3} \Psi_\alpha^{\alpha'} \Phi_{ij\alpha}^{mn\alpha'} \big[\cos(\Delta_\alpha^{mn} + x_\alpha)\cos(\Delta_{ij}^{\alpha'} - y_\alpha^{\alpha'}) + \sin(\Delta_\alpha^{mn})\sin(\Delta_{ij}^{\alpha'} + z_\alpha^{\alpha'})\big], \tag{17}$$

where

$$\Psi_\alpha^{\alpha'} = \begin{cases} \dfrac{|p_\alpha|}{2\mathrm{Im}^2[p_\alpha]} & \text{if } \alpha = \alpha' \\[2ex] \dfrac{|p_\alpha|}{\mathrm{Im}[p_\alpha]}\left[\dfrac{\mathcal{F}(p_\alpha)}{\mathcal{Q}(p_\alpha)}\right]^{1/2} & \text{if } \alpha \neq \alpha' \end{cases}$$

$$\Phi_{ij\alpha}^{mn\alpha'} = 2|A_{i\alpha}||A_{m\alpha'}||D_\alpha||D_{\alpha'}||p_\alpha|^{j-1}|p_{\alpha'}|^{n-1}. \tag{18}$$

Explicit expressions for $\mathcal{F}(p_\alpha)$, $\mathcal{Q}(p_\alpha)$, x_α, $y_\alpha^{\alpha'}$, $z_\alpha^{\alpha'}$ and Δ_α^{mn} are reported in Appendix *A*. The complex quantities p_α and $(\mathbf{A}_\alpha, \mathbf{L}_\alpha)$ are the eigensolutions of the fundamental elasticity matrix N (Ting, 1996), obeying the eigenrelation

$$N\begin{bmatrix}\mathbf{A}_\alpha \\ \mathbf{L}_\alpha\end{bmatrix} = p_\alpha \begin{bmatrix}\mathbf{A}_\alpha \\ \mathbf{L}_\alpha\end{bmatrix}. \tag{19}$$

Once the elastic eigenproblem in equation (19) is solved and therefore the eigensolutions p_α and $(\mathbf{A}_\alpha, \mathbf{L}_\alpha)$ are known, equations (17) and (18) provide the solution for E_{ijmn} without recourse to the numerical methods used in the literature to date to solve the integral in equation (12).

Moreover, when dislocations are favorably oriented with respect to the symmetry axes of the unit cell, analytical eigensolutions can be obtained. Equation (17) can then be reduced to simple polynomial functions of the crystal's elastic properties (Martinez-Garcia *et al.*, 2007, 2008).

Equations (11) and (17) are the general solutions for G_{ijmn} and E_{ijmn} which, inserted in equation (9), allow a direct determination of the contrast factor of dislocations of any slip system.

2.3. Average contrast factor

In the case of polycrystalline materials with randomly oriented grains, the dislocation contrast factor has to be averaged over the N crystallographically equivalent (*i.e.* indistinguishable from a powder point of view) slip systems,

$$\overline{C}_{hkl} = (1/N)\sum_{i}^{N} C_{hkl}^{i}, \tag{20}$$

C_{hkl}^{i} being the contrast factor corresponding to the ith slip system. Therefore, a prerequisite to the determination of $\overline{C}_{hkl}$ is the generation of all S reference frames equivalent to a given one.

In the previous section it was shown how to build S in the general case, given the unit-cell parameters, slip plane, Burgers vector and dislocation character. The minimum requirement for finding the set of equivalent slip systems is knowledge of the symmetry operations sufficient to obtain any vector equivalent to a given one [*i.e.* the Laue point group for the given lattice (Sands, 1982)].

The required symmetry information (point group and Bravais lattice) is contained in the three-dimensional space group. In particular, the space-group generators obtained from the space-group symbol [using the procedure of Shmueli (1984)] allow all slip systems equivalent to a given one to be evaluated. In fact, only a subset of point-group operations is needed. The point-group operators and unit vectors $\{\mathbf{e}_k;\, k = 1, 2, 3\}$, suitably referred to the common O frame, are used to generate all equivalent slip systems.

The number of calculations can be reduced by considering that $(\mathbf{b}_v, \mathbf{l})$ and $(-\mathbf{b}_v, -\mathbf{l})$ represent the same straight-line dislocation and thus $\{\mathbf{e}_1, \mathbf{e}_2, \mathbf{e}_3\}$, $\{-\mathbf{e}_1, -\mathbf{e}_2, \mathbf{e}_3\}$, $\{-\mathbf{e}_1, \mathbf{e}_2, -\mathbf{e}_3\}$ and $\{\mathbf{e}_1, -\mathbf{e}_2, -\mathbf{e}_3\}$ are crystallographically equivalent slip coordinate systems (Bollman, 1970).

Sets of equivalent S coordinate systems for the most common slip systems are tabulated in Martinez-Garcia (2008).

The average contrast factor can finally be calculated by means of equations (20), (17), (11) and (9). To further help the reader, Fig. 2 shows a schematic representation of the whole procedure.

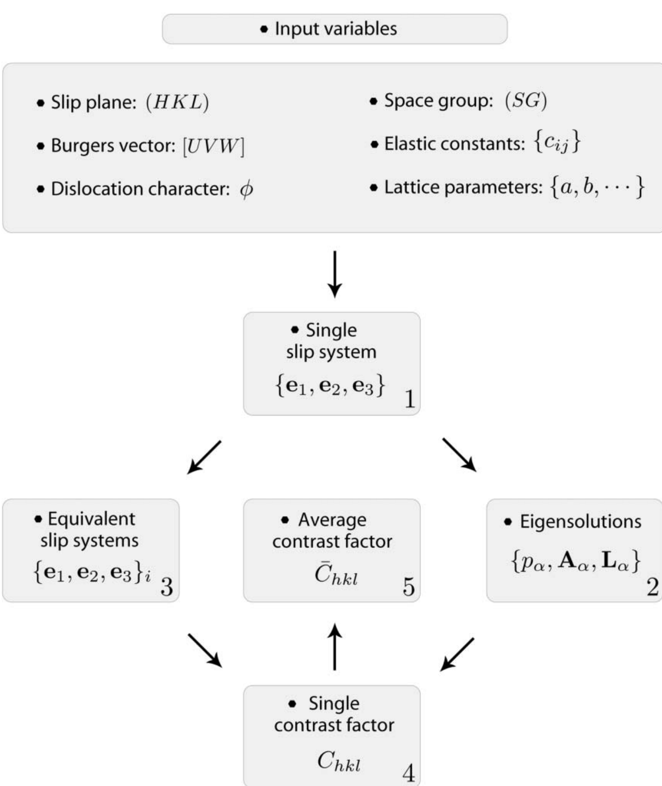

Figure 2
Schematic representation of the algorithm proposed for the average contrast factor computation. Input variables are used to build a single slip coordinate system on the dislocation line (1), in which the elastic eigenproblem is solved (2). Space-group information is used to generate all crystallographically equivalent slip coordinate systems (3). The eigensolutions are used to evaluate single contrast factors for each member of the equivalent slip coordinate system set (4). Finally an average contrast factor is determined (5).

Table 1
Anisotropic elastic constants (GPa) and c/a ratio for Zn and Mg.

Material	c_{11}	c_{12}	c_{13}	c_{33}	c_{44}	c/a
Zn	165.0	31.0	50.0	62.0	39.6	1.86
Mg	59.2	25.7	21.4	61.4	16.4	1.62

3. Applications

3.1. Comparison with previous works

A comparison with previous results is only possible for some materials with cubic or hexagonal symmetry, as there are no literature data on lower-symmetry phases. The proposed procedure was thus applied to several cases of slip systems in cubic or hexagonal metals and compared with results from *ANIZC* (Borbély *et al.*, 2003) or those published by KK (Klimanek & Kužel, 1988; Kužel & Klimanek, 1988).

By employing both the elastic constants and the c/a ratios listed in Table 1 for Zn and Mg, the geometrical (G_{ijmn}) and elastic (E_{ijmn}) components of $\overline{C}_{hkl}$ were determined numerically for the most common slip systems reported for hexagonal lattices (Klimanek & Kužel, 1988). Averaged contrast factors were then determined by using equations (9) and (20).

To compare our results with those of KK, average contrast factors for Mg and Zn are shown in Fig. 3 as a function of δ, the angle between the diffraction vector $\mathbf{d}^*$ and the c axis of the hexagonal lattice:

$$\cos\delta = \frac{(3/2)^{1/2}(a/c)l}{[2(h^2+hk+k^2)+(3/2)(a/c)^2\,l^2]^{1/2}}. \qquad (21)$$

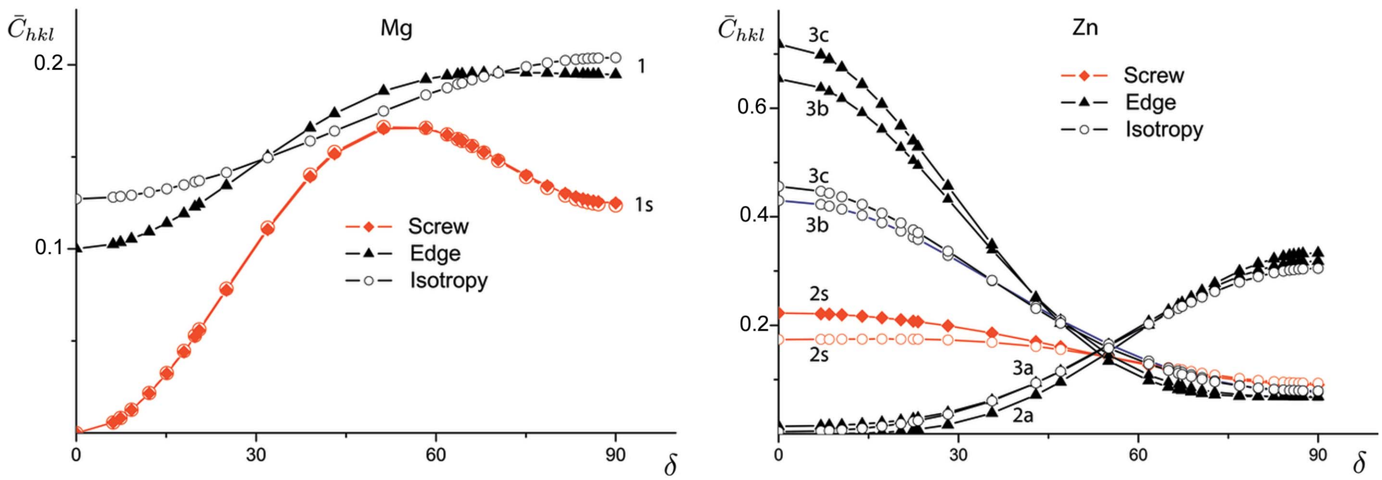

(*a*) (*b*)

Figure 3
Dependence of the average contrast factor, $\overline{C}_{hkl}$ on the angle δ between the diffraction vector $\mathbf{d}^*$ and the c axis of the hexagonal unit cell for (*a*) Mg and (*b*) Zn. Slip systems are identified as in Klimanek & Kužel (1988) and Kužel & Klimanek (1988) with a number–letter code. Screw: 1s $1/3\langle 2\bar{1}\bar{1}0\rangle\{0001\}$, 2s $1/3\langle\bar{2}113\rangle\{01\bar{1}0\}$; edge: 1 $1/3\langle 2\bar{1}\bar{1}0\rangle\{0001\}$, 2a $1/3\langle 2\bar{1}\bar{1}0\rangle\{01\bar{1}0\}$, 3a $1/3\langle 2\bar{1}\bar{1}0\rangle\{01\bar{1}1\}$, 3b $1/3\langle 2\bar{1}\bar{1}3\rangle\{10\bar{1}1\}$ and 3c $1/3\langle 2\bar{1}\bar{1}3\rangle\{2\bar{1}\bar{1}2\}$. Open circles correspond to the calculations done under the elastic isotropy approximation.

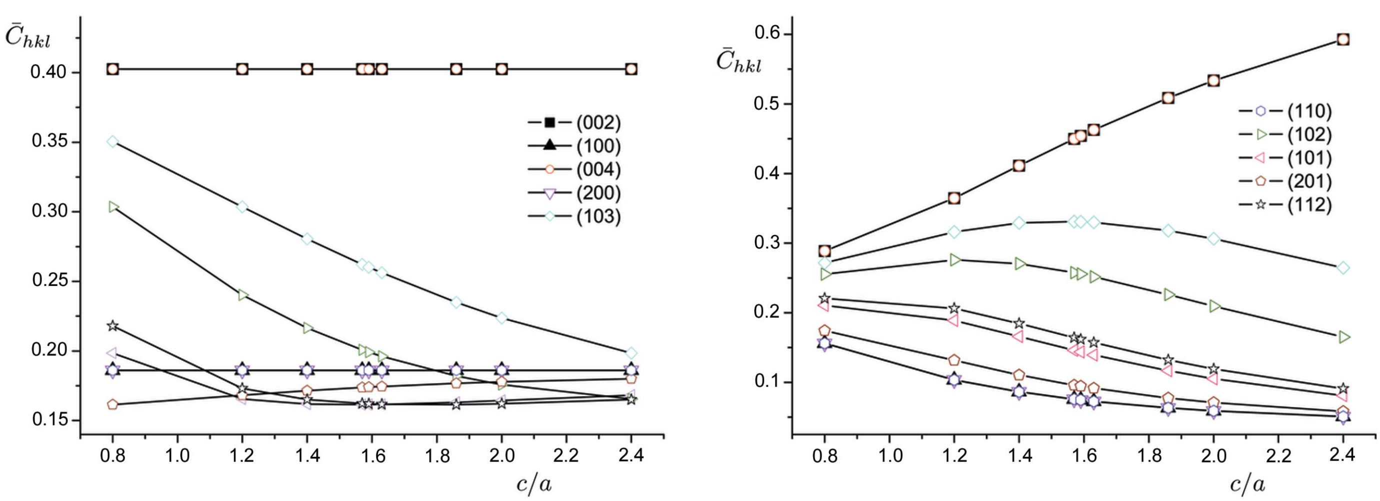

(*a*) (*b*)

Figure 4
Dependence of the average contrast factor, $\overline{C}_{hkl}$, of edge dislocations on the c/a ratio for some typical reflections. (*a*) $1/3\langle 2\bar{1}\bar{1}0\rangle\{0001\}$ basal slip system. (*b*) $1/3\langle\bar{2}113\rangle\{11\bar{2}1\}$ pyramidal slip system.

Table 2
Eigenvalues and elastic component for edge and screw dislocations in α-Mg_2SiO_4 for the $\langle 100\rangle\{010\}$ slip system.

Character	p_1	p_2	p_3	E
Edge	$1.543i$	$0.829i$	$1.104i$	
				$\begin{bmatrix} 0.473 & 0 & 0 & 0 & -0.079 & 0 \\ & 0.605 & 0 & -0.868 & 0 & 0 \\ & & 0 & 0 & 0 & 0 \\ & & & 2.189 & 0 & 0 \\ & & & & 0.134 & 0 \\ & & & & & 0 \end{bmatrix}$
Screw	$1.306i$	$0.830i$	$1.002i$	
				$\begin{bmatrix} 0 & 0 & 0 & 0 & 0 & 0 \\ & 0 & 0 & 0 & 0 & 0 \\ & & 0.997 & 0 & 0 & 0 \\ & & & 0 & 0 & 0 \\ & & & & 0 & 0 \\ & & & & & 1.002 \end{bmatrix}$

Table 3
Eigenvalues and elastic component for edge and screw dislocations in α-Mg_2SiO_4 for the $\langle 001\rangle\{100\}$ slip system.

Character	p_1	p_2	p_3	E
Edge	$1.385i$	$0.611i$	$0.908i$	
				$\begin{bmatrix} 0.561 & 0 & 0 & 0 & -0.055 & 0 \\ & 0.475 & 0 & -0.692 & 0 & 0 \\ & & 0 & 0 & 0 & 0 \\ & & & 1.834 & 0 & 0 \\ & & & & 0.065 & 0 \\ & & & & & 0 \end{bmatrix}$
Screw	$1.205i$	$0.648i$	$0.906i$	
				$\begin{bmatrix} 0 & 0 & 0 & 0 & 0 & 0 \\ & 0 & 0 & 0 & 0 & 0 \\ & & 1.104 & 0 & 0 & 0 \\ & & & 0 & 0 & 0 \\ & & & & 0 & 0 \\ & & & & & 0.906 \end{bmatrix}$

The results shown in Fig. 3 match those reported by KK very well [see Figs. 1*a* and *b* in Kužel & Klimanek (1988)], the only slight difference being visible for the $1/3\langle\overline{2}113\rangle\{01\overline{1}0\}$ (2s) slip system in the case of elastically anisotropic Zn. Further discrepancies with the KK results are reported in Martinez-Garcia (2008).

As expected, there are large differences among the shapes of the $\overline{C}_{hkl} = f(\delta)$ functions associated with different slip systems and/or dislocation characters (*i.e.* edge and screw orientations).

Using these numerical results, the influence of the *c*/*a* ratio on $\overline{C}_{hkl}$ for some typical reflections *hkl* was also investigated. Fig. 4 shows the dependence of $\overline{C}_{hkl}$ on the *c*/*a* ratio for the $1/3\langle 2\overline{1}\overline{1}0\rangle\{0001\}$ and $1/3\langle\overline{2}113\rangle\{11\overline{2}1\}$ slip systems taking into account dislocations with edge orientations. It is interesting to see how the values of $\overline{C}_{hkl}$ (thus the diffraction broadening) varies with the *c*/*a* ratio. Changes in the contrast-factor behavior are particularly evident for the (*h*00), (*hh*0) and (00*l*) reflections, where values are deeply influenced by dislocation geometry changes, *e.g.* from basal $1/3\langle 2\overline{1}\overline{1}0\rangle\{0001\}$ to pyramidal $1/3\langle\overline{2}113\rangle\{11\overline{2}1\}$ slip.

3.2. Lower-symmetry minerals

3.2.1. Forsterite (α-Mg_2SiO_4). Forsterite is one of the dominant minerals in the upper mantle of the Earth (30 to 410 km depth). Its rheological behavior is therefore crucial for the understanding of the deformation processes at a depth where the convective flow of the mantle is coupled to the movement of the lithospheric plates that constitute the uppermost 100 km of the Earth's crust. The development of texture and consequent anisotropy of physical parameters during plastic deformation of forsterite is of special interest, since they can be directly compared to geophysical observations of seismic wave velocities.

Table 4
Eigenvalues and elastic component for edge and screw dislocations in α-Mg_2SiO_4 for the $\langle 001\rangle\{010\}$ slip system.

Character	p_1	p_2	p_3	E
Edge	$1.306i$	$0.830i$	$1.002i$	$\begin{bmatrix} 0.517 & 0 & 0 & 0 & -0.117 & 0 \\ & 0.561 & 0 & -0.791 & 0 & 0 \\ & & 0 & 0 & 0 & 0 \\ & & & 2.023 & 0 & 0 \\ & & & & 0.119 & 0 \\ & & & & & 0 \end{bmatrix}$
Screw	$1.543i$	$0.829i$	$1.104i$	$\begin{bmatrix} 0 & 0 & 0 & 0 & 0 & 0 \\ & 0 & 0 & 0 & 0 & 0 \\ & & 0.906 & 0 & 0 & 0 \\ & & & 0 & 0 & 0 \\ & & & & 0 & 0 \\ & & & & & 1.104 \end{bmatrix}$

Forsterite is orthorhombic (space group *Pbnm*), with cell parameters $a = 4.775$, $b = 10.190$ and $c = 5.978$ Å. The structure is usually described as the coupling between SiO_4^{2-} tetrahedra and Mg^{2+} cations (Fig. 5*a*) (Fujino *et al.*, 1981). Elastic constants for this mineral have been reported by Bass (1995).

Slip systems reported in the literature for this mineral are $\langle 100\rangle\{010\}$, $\langle 001\rangle\{hk0\}$ and $\langle 100\rangle\{001\}$ (Bai *et al.*, 1991; Nicolas *et al.*, 1973; Raleigh, 1968). According to equation (11), the $\{\tau_k, k = 1, 2, 3\}$ elements in the case of edge orientation have the form

$$\begin{aligned} \tau_1 &= \frac{h}{[h^2 + (a/b)^2k^2 + (a/c)^2l^2]^{1/2}} \\ \tau_2 &= \frac{(a/b)k}{[h^2 + (a/b)^2k^2 + (a/c)^2l^2]^{1/2}} \\ \tau_3 &= \frac{(a/c)l}{[h^2 + (a/b)^2k^2 + (a/c)^2l^2]^{1/2}}, \end{aligned} \tag{22}$$

$$\begin{aligned} \tau_1 &= \frac{(a/c)l}{[h^2 + (a/b)^2k^2 + (a/c)^2l^2]^{1/2}} \\ \tau_2 &= \frac{h}{[h^2 + (a/b)^2k^2 + (a/c)^2l^2]^{1/2}} \\ \tau_3 &= \frac{(a/b)k}{[h^2 + (a/b)^2k^2 + (a/c)^2l^2]^{1/2}} \end{aligned} \tag{23}$$

and

$$\begin{aligned} \tau_1 &= \frac{(a/c)l}{[h^2 + (a/b)^2k^2 + (a/c)^2l^2]^{1/2}} \\ \tau_2 &= \frac{(a/b)k}{[h^2 + (a/b)^2k^2 + (a/c)^2l^2]^{1/2}} \\ \tau_3 &= -\frac{h}{[h^2 + (a/b)^2k^2 + (a/c)^2l^2]^{1/2}} \end{aligned} \tag{24}$$

for $\langle 100\rangle\{010\}$, $\langle 001\rangle\{100\}$ and $\langle 001\rangle\{010\}$, respectively. The τ values can be used to determine the symmetrical matrix G, defining the geometrical component of the contrast factor. Direction cosines for screw orientations can be obtained from the edge counterparts by exchanging $(\tau_1 \rightarrow -\tau_3)$ and $(\tau_3 \rightarrow \tau_1)$.

The elastic component of the contrast factor, E, can be determined by using equations (17) and (18), once the Stroh eigenvalue problem [*cf.* equation (19)] has been solved. Following this approach, both the eigenvalues p_α and the matrix E of forsterite were numerically calculated. Results are

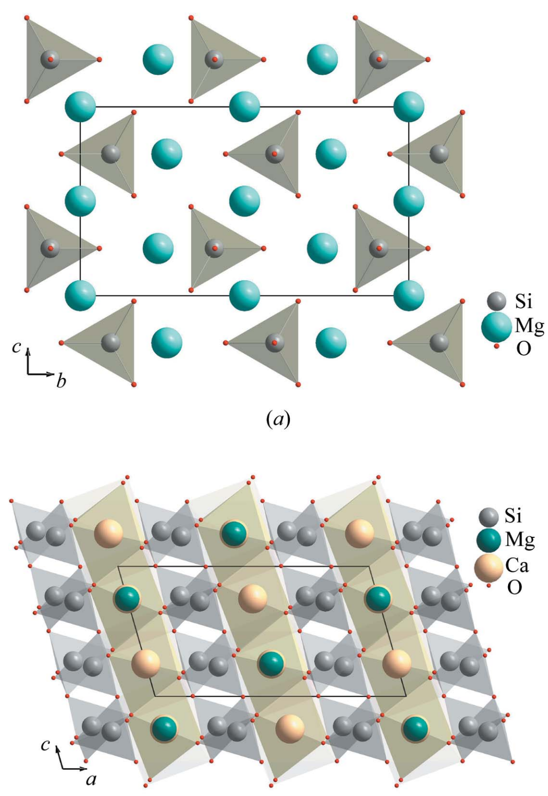

(*b*)

Figure 5
Projections along the *a* and *b* axes of the structures of (*a*) forsterite, α-Mg_2SiO_4, and (*b*) diopside, $CaMgSi_2O_6$, respectively.

Table 5
Average contrast factor for edge and screw dislocations in α-Mg_2SiO_4 for the $\langle 100\rangle\{010\}$ slip system.

Lattice parameters: a = 4.775, b = 10.190, c = 5.978 Å; elastic stiffnesses: C_{11} = 328, C_{22} = 200, C_{33} = 235, C_{44} = 66.7, C_{55} = 81.3, C_{66} = 80.9, C_{12} = 69, C_{13} = 69, C_{23} = 73 GPa.

	$\overline{C}_{hkl}$			$\overline{C}_{hkl}$	
hkl	Edge	Screw	*hkl*	Edge	Screw
020	0.1340	0	150	0.2248	0.1315
110	0.4548	0.1471	202	0.1773	0.2367
021	0.0449	0	113	0.0141	0.1235
101	0.1773	0.2367	151	0.1864	0.1216
111	0.1970	0.2480	222	0.1970	0.2480
120	0.3876	0.2494	240	0.3876	0.2494
121	0.2165	0.2400	123	0.0237	0.1145
002	0	0	241	0.3295	0.2503
130	0.3137	0.2243	061	0.1147	0
131	0.2129	0.2012	232	0.2097	0.2491
112	0.0480	0.1952	133	0.0367	0.1021
041	0.0960	0	160	0.2016	0.1006
210	0.4693	0.0490	152	0.1159	0.0991

Table 6
Average contrast factor for edge and screw dislocations in α-Mg_2SiO_4 for the $\langle 001\rangle\{100\}$ slip system.

	$\overline{C}_{hkl}$			$\overline{C}_{hkl}$	
hkl	Edge	Screw	*hkl*	Edge	Screw
020	0	0	150	0.0015	0
110	0.0440	0	202	0.3022	0.2149
021	0.0993	0.2690	113	0.4793	0.1366
101	0.3022	0.2149	151	0.01610	0.0873
111	0.2353	0.2117	222	0.2353	0.2117
120	0.0186	0	240	0.01864	0
121	0.1285	0.1884	123	0.4001	0.1858
002	0.5611	0	241	0.0506	0.0717
130	0.0074	0	061	0.0031	0.0762
131	0.0624	0.1504	232	0.1788	0.2030
112	0.4072	0.2064	133	0.3058	0.2333
041	0.0132	0.1436	160	0.008	0
210	0.0586	0	152	0.0710	0.2172

reported in Tables 2, 3 and 4 for $\langle 100\rangle\{010\}$, $\langle 001\rangle\{100\}$ and $\langle 001\rangle\{010\}$, respectively, for the cases of screw and edge orientations.

Average contrast-factor values for forsterite were then numerically determined by using the above results together with equations (20) and (9). Tables 5, 6 and 7 show forsterite $\overline{C}_{hkl}$ values calculated for the major reflections and for each of the investigated slip systems. The lattice parameters and elastic constants used in the calculations are also given in Table 5.

3.2.2. Muscovite and diopside. Among the materials showing monoclinic symmetry, diopside ($CaMgSi_2O_6$) and muscovite [$KAl_3Si_3O_{10}(OH)_2$] are minerals whose plastic properties have been thoroughly examined in the literature (Bass, 1995).

Diopside is an important rock-forming mineral of the pyroxene group, crystallizing in space group $C2/c$ with unit-cell parameters a = 9.746, b = 8.899, c = 5.251 Å and β = 105.63° (Anthony *et al.*, 2003) (Fig. 5*b*). Muscovite is the most common mica and is typically found as massively crystalline material in 'books' or in flaky grains as a constituent of many rocks. It also crystallizes in space group $C2/c$ and is composed of aluminium silicate sheets weakly bonded together by layers of potassium ions. The unit-cell parameters for muscovite are a = 5.19, b = 9.04, c = 20.08 Å, β = 95.5° (Fig. 6) (Anthony *et al.*, 2003).

Table 7
Average contrast factor for edge and screw dislocations in α-Mg_2SiO_4 for the $\langle 001\rangle\{010\}$ slip system.

	$\overline{C}_{hkl}$			$\overline{C}_{hkl}$	
hkl	Edge	Screw	*hkl*	Edge	Screw
020	0.1198	0	150	0.0855	0
110	0.0038	0	202	0.0775	0.2149
021	0.3184	0.2690	113	0.3708	0.1366
101	0.0775	0.2149	151	0.1277	0.0873
111	0.0928	0.2117	222	0.0928	0.2117
120	0.0259	0	240	0.0259	0
121	0.1147	0.1884	123	0.3608	0.1858
002	0.5171	0	241	0.0508	0.0717
130	0.0525	0	061	0.1584	0.0762
131	0.1252	0.1504	232	0.1094	0.2030
112	0.2660	0.2064	133	0.3440	0.2333
041	0.1976	0.1436	160	0.9427	0
210	0.0003	0	152	0.2161	0.2172

The major slip systems reported in the literature for these minerals are [001](100) for diopside (Kollé & Blacic, 1982), and [100](001) and [110](001) for muscovite (Meike, 1989).

Direction cosines can be determined for these minerals by using equation (11). For example, for dislocation lines with screw orientation in muscovite (β = 95.5°), the $\{\tau_k;\, k = 1, 2, 3\}$ elements in equation (11) take the form

$$\tau_1 = \frac{[1+(b/a)^2]^{-3/2}[(b/a)^3h-(a/b)k-(b/a)(h-k)]}{[1.009h^2+(a/b)^2k^2+0.193(a/c)hl+1.009(a/c)^2l^2]^{1/2}}$$
$$\tau_2 = \frac{0.096h+1.004(a/c)l}{[1.009h^2+(a/b)^2k^2+0.193(a/c)hl+1.009(a/c)^2l^2]^{1/2}}$$
$$\tau_3 = \frac{[1+(b/a)^2]^{-1/2}(h+k)}{[1.009h^2+(a/b)^2k^2+0.193(a/c)hl+1.009(a/c)^2l^2]^{1/2}}$$

for the [110](001) slip system.

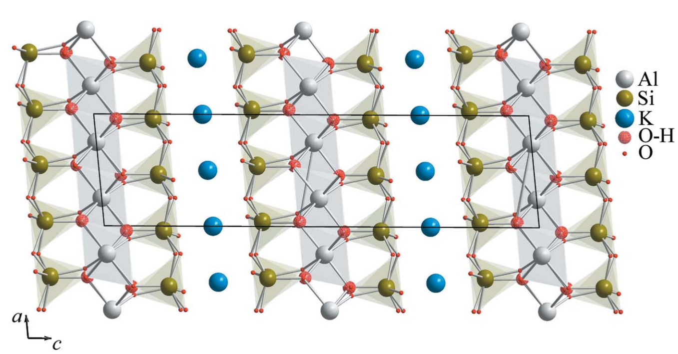

Figure 6
Projection along the b axis of the structure of muscovite, $KAl_3Si_3O_{10}(OH)_2$. The structure is formed from a sandwich of two tetrahedral layers composed of sheets of linked $Si^{4+}O_4^{2-}$ tetrahedra joined by a layer of Al^{3+} ions octahedrally coordinated by O atoms and O—H groups. Single layers of K^+ cations appear between two tetrahedral layers.

Table 8
Eigenvalues and elastic component for edge and screw dislocations in diopside for the [001](100) slip system.

Character	p_1	p_2	p_3	E
Edge	$0.081 + 1.709i$	$0.105 + 0.702i$	$0.162 + 1.056i$	$\begin{bmatrix} 0.4491 & -0.0306 & 0 & 0.0767 & -0.1465 & 0 \\ & 0.5469 & 0 & -0.7748 & 0.0075 & 0 \\ & & 0 & 0 & 0 & 0 \\ & & & 2.3396 & 0.053 & 0 \\ & & & & 0.1386 & 0 \\ & & & & & 0 \end{bmatrix}$
Screw	$0.375 + 0.989i$	$-0.375 + 0.989i$	$1.019i$	$\begin{bmatrix} 0.018 & 0 & 0 & 0 & -0.002 & 0.125 \\ & 0 & -0.004 & -0.002 & 0 & 0 \\ & & 0.844 & 0.044 & 0 & 0 \\ & & & 0.013 & 0 & 0 \\ & & & & 0.001 & 0.0045 \\ & & & & & 1.184 \end{bmatrix}$

Table 9
Eigenvalues and elastic component for edge and screw dislocations in muscovite for the [100](001) slip system.

Character	p_1	p_2	p_3	E
Edge	$0.178 + 2.961i$	$-0.037 + 0.594i$	$-0.031 + 2.127i$	$\begin{bmatrix} 0.304 & 0 & 0 & 0.039 & -0.073 & 0 \\ & 0.538 & 0 & -0.838 & 0.006 & 0 \\ & & 0 & 0 & 0 & 0 \\ & & & 3.334 & -0.066 & 0 \\ & & & & 0.112 & 0 \\ & & & & & 0 \end{bmatrix}$
Screw	$3.0853i$	$2.0384i$	$0.5606i$	$\begin{bmatrix} 0 & 0 & 0 & 0 & 0 & -0.034 \\ & 0 & 0.003 & 0 & 0 & 0 \\ & & 0.492 & 0.006 & 0 & 0 \\ & & & 0 & 0 & 0 \\ & & & & 0 & -0.011 \\ & & & & & 2.032 \end{bmatrix}$

Direction cosines for edge orientations can be obtained from the screw ones by exchanging $(\tau_1 \rightarrow -\tau_3)$ and $(\tau_3 \rightarrow \tau_1)$. By means of the above expressions, the geometrical component of the contrast factor, G, can be readily determined.

Tables 8 and 9 show the numerically calculated eigenvalues and the E matrices for the [001](100) and [100](001) slip systems in diopside and muscovite, respectively. Both screw and edge orientations were assumed.

It is worth emphasizing that, in this case, each slip system is only crystallographically equivalent to itself, as prescribed by the point group $2/m$. Thus, only single contrast factors need to be considered.

Taking into account the above results and inserting the calculated matrices G and E in equation (9), the contrast factors for diopside and muscovite were calculated as a function of the Miller indices. Fig. 7 shows the dependence of the contrast factor on the angle δ for (*a*) the [001](100) slip system in diopside and (*b*, *c*) for the [100](001) and [110](001) slip systems in muscovite, respectively. Here δ is the angle between $\mathbf{d}^*$ and the b axis of the monoclinic lattice (on the $\{\mathbf{a} + \mathbf{c}, \mathbf{b}\}$ plane), calculated as

$$\delta = (a/b)k\Big\{\big[h^2 + (a/b)^2k^2 + (a/c)^2l^2\big]\csc^2(\beta) - (a/b)^2k^2\cot^2(\beta) - 2(a/c)hl\cot(\beta)\csc(\beta)\Big\}^{-1/2}. \quad (25)$$

As can be seen from Fig. 7(*c*), the elastic anisotropy is quite strong for muscovite in the [110](100) slip system for both screw and edge orientations. This is a typical example where the effect of the elastic anisotropy cannot be neglected.

4. Conclusions

The dislocation contrast factor is the main parameter representing the anisotropic nature of the dislocation strain field and its effects on diffraction phenomena. Until now, the evaluation of this important parameter has been an *ad hoc* procedure, specific for materials showing cubic and hexagonal symmetry, and carried out through numerical calculations.

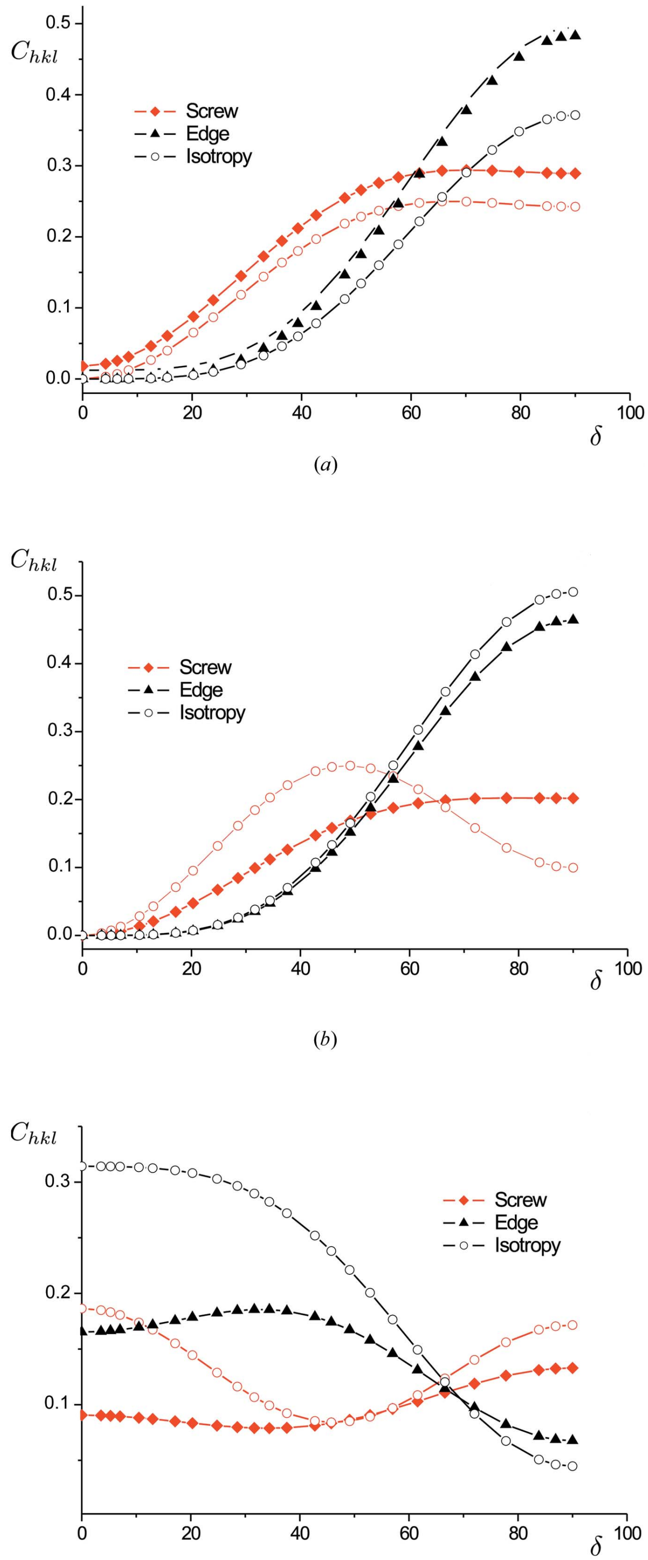

Figure 7
Dependence of C_{hkl} on the angle δ between $\mathbf{d}^*$ and the b axis of the monoclinic lattice for screw and edge orientations. (*a*) [001](100) slip system for diopside. (*b*) [100](001) slip system for muscovite. (*c*) [110](001) slip system for muscovite. Open circles correspond to the calculations using the elastic isotropy approximation. The Poisson-ratio values used were $\nu = 0.26$ for diopside and $\nu = 0.25$ for muscovite (Bass, 1995).

In this paper a new general approach for evaluating the dislocation contrast factor is presented and used. It extends the Klimanek–Kužel procedure to any crystal, independently of its symmetry and elastic properties. The results agree with the literature data for cubic and hexagonal materials. Applications shown for low-symmetry phases are new and demonstrate the generality of the proposed approach.

APPENDIX *A*
Elastic component: useful formulae

The analytical expressions for the parameters which appear in equations (17) and (18) are

$$\begin{aligned}
\mathcal{F}(p_\alpha) &= (\mathrm{Re}[p_\alpha] - \mathrm{Re}[p_{\alpha'}])^2 + (\mathrm{Im}[p_\alpha] - \mathrm{Im}[p_{\alpha'}])^2,\\
\mathcal{Q}(p_\alpha) &= (|p_\alpha|^2 - |p_{\alpha'}|^2)^2 + 4(\mathrm{Re}[p_\alpha] - \mathrm{Re}[p_{\alpha'}])\\
&\quad \times (|p_{\alpha'}|^2 \mathrm{Re}[p_\alpha] - |p_\alpha|^2 \mathrm{Re}[p_{\alpha'}]),\\
x_\alpha &= \arctan\left(\frac{\mathrm{Re}[p_\alpha]}{\mathrm{Im}[p_\alpha]}\right),\\
y_\alpha^{\alpha'} &= \arctan\left(\frac{\mathrm{Re}[p_\alpha] - \mathrm{Re}[p_{\alpha'}]}{\mathrm{Im}[p_\alpha] + \mathrm{Im}[p_{\alpha'}]}\right),\\
z_\alpha^{\alpha'} &= \arctan\left(\frac{\Gamma_1(\alpha)}{\Gamma_2(\alpha)}\right),\\
\Delta_\alpha^{mn} &= \arg(A_{m\alpha}\, D_\alpha\, p_\alpha^{n-1}),
\end{aligned} \tag{26}$$

where

$$\begin{aligned}
\Gamma_1(\alpha) &= \mathrm{Im}[p_\alpha]\mathrm{Im}[p_{\alpha'}][\tan(x_\alpha) + \tan(x_{\alpha'})],\\
\Gamma_2(\alpha) &= |p_\alpha|^2 - \mathrm{Re}[p_\alpha]\mathrm{Re}[p_{\alpha'}] + \mathrm{Im}[p_\alpha]\mathrm{Im}[p_{\alpha'}],
\end{aligned} \tag{27}$$

Re[] and Im[] being the real and imaginary part operators, respectively.

We thank Professor Ernesto Estévez Rams for useful discussions and suggestions. This research was carried out while JM-G was a PhD student at the University of Trento within the frame of an international agreement with the University of Havana. JM-G is particularly grateful to both universities for making possible the successful realization of this project.

References

Anthony, J. W., Bideaux, R. A., Bladh, K. W. & Nichols, M. C. (2003). *Handbook of Mineralogy*. Tucson: Mineral Data Publishing.

Armstrong, N., Leoni, M. & Scardi, P. (2006). *Z. Kristallogr. Suppl.* **23**, 81–86.

Armstrong, N. & Lynch, P. (2004). *Diffraction Analysis of the Microstructure of Materials*, edited by E. Mittemeijer & P. Scardi, pp. 249–286. Berlin: Springer-Verlag.

Bai, Q., Mackwell, S. J. & Kohlstedt, D. L. (1991). *J. Geophys. Res.* **96**(B2), 2441–2463.

Bass, J. D. (1995). *Mineral Physics and Crystallography: A Handbook of Physical Constants*, edited by T. J. Ahrens, pp. 45–63. Washington: American Geophysical Union.

Bollman, W. (1970). *Crystal Defects and Crystalline Interfaces*. New York: Springer-Verlag.

Borbély, A., Dragomir-Cernatescu, J., Ribárik, G. & Ungár, T. (2003). *J. Appl. Cryst.* **36**, 160–162.

Dragomir, I. C. & Ungár, T. (2002*a*). *J. Appl. Cryst.* **35**, 556–564.

Dragomir, I. C. & Ungár, T. (2002*b*). *Powder Diffr.* **17**, 104–111.

Fujino, K., Sasaki, S., Takéuchi, Y. & Sadanaga, R. (1981). *Acta Cryst.* B**37**, 513–518.

Giacovazzo, C., Monaco, H. L., Artioli, G., Viterbo, D., Ferraris, G., Gilly, G., Zanotti, G. & Catti, M. (1992). *Fundamentals of Crystallography*, 2nd ed. Oxford University Press.

Klimanek, P. & Kužel, R. (1988). *J. Appl. Cryst.* **21**, 59–66.

Kollé, J. J. & Blacic, J. D. (1982). *J. Geophys. Res.* **87**(B5), 4019–4034.

Krivoglaz, M. A., Martynenko, O. V. & Ryaboshapka, K. P. (1983). *Fiz. Met. Metalloved.* **55**, 5–17.

Krivoglaz, M. A. & Ryaboshapka, K. P. (1963). *Fiz. Met. Metalloved.* **15**, 18–31.

Kužel, R. & Klimanek, P. (1988). *J. Appl. Cryst.* **21**, 363–368.

Lekhnitskii, S. G. (1963). *Theory of Elasticity of an Anisotropic Elastic Body*. San Francisco: Holden-Day.

Martinez-Garcia, J. (2008). *The X-ray Contrast Factor of Straight-line Dislocations*. PhD thesis, University of Trento. ISBN 978-88-8443-263-6.

Martinez-Garcia, J., Leoni, M. & Scardi, P. (2007). *Phys. Rev. B*, **76**, 174117.

Martinez-Garcia, J., Leoni, M. & Scardi, P. (2008). *Philos. Mag. Lett.* **88**, 443–451.

Meike, A. (1989). *Am. Mineral.* **74**, 780–796.

Mittemeijer, E. J. & Scardi, P. (2004). Editors. *Diffraction Analysis of the Microstructure of Materials*. Berlin: Springer-Verlag.

Nicolas, A., Boudier, F. & Boulier, A. M. (1973). *Am. J. Sci.* **10**, 853–876.

Raleigh, C. B. (1968). *J. Geophys. Res.* **73**, 5391–5406.

Ryaboshapka, K. P. (1965). *Metal Physics. Imperfections in Crystal Structure*, p. 3. Kiev: Naukova Dumka Izd. Akad. Nauk Ukr. SSR.

Sands, D. E. (1982). *Vectors and Tensors in Crystallography*. Reading: Addison-Wesley.

Shmueli, U. (1984). *Acta Cryst.* A**40**, 559–567.

Stroh, A. N. (1958). *Philos. Mag.* **3**, 625–646.

Stroh, A. N. (1962). *J. Math. Phys.* **41**, 77–103.

Teodosiou, C. (1982). *Elastic Models of Crystal Defects*. New York: Springer-Verlag.

Ting, T. C. (1996). *Anisotropic Elasticity: Theory and Applications*. New York, Oxford: Oxford University Press.

Ungár, T., Dragomir, I., Révész, Á. & Borbély, A. (1999). *J. Appl. Cryst.* **32**, 992–1002.

Wilkens, M. (1970*a*). *Phys. Status Solidi A*, **2**, 359–370.

Wilkens, M. (1970*b*). *Fundamental Aspects of Dislocation Theory*, edited by J. A. Simmons, R. de Wit & R. Bullough, Vol. II, pp. 1195–1221. National Bureau of Standards Special Publication No. 317. Washington: National Bureau of Standards.

Wilkens, M. (1987). *Phys. Status Solidi A*, **104**, K1–K6.

Williamson, G. K. & Hall, W. H. (1953). *Acta Metall.* **1**, 22–31.

Wilson, A. J. C. (1949). *Res. London*, **2**, 541.

Wilson, A. J. C. (1950). *Res. London*, **3**, 387.